Punching Shear of Reinforced Concrete Slabs under Fire Conditions: Experiment vs. Design

PUNCHING SHEAR OF REINFORCED CONCRETE SLABS UNDER FIRE CONDITIONS: EXPERIMENT VS. DESIGN

A. Holly K. M. Smith, *The University of Edinburgh and AECOM, UK*
B. T. Stratford & **L. Bisby**, *The University of Edinburgh, UK*

ABSTRACT

Shear behaviour in concrete at ambient temperature is complex, and a well-researched topic. There is even less knowledge about shear in concrete subjected to the thermal gradients due to fire, with only a few experimental studies having been conducted. Fifteen model slab-column punching shear specimens were tested at both ambient and elevated temperature. These tests are some of the first to have compared the effects of different support conditions, which aimed to replicate whole structural behaviour. This paper has presented a comparison of experimental data from a punching shear test series to both Eurocode design and Muttoni's Critical Shear Crack Theory. The analysis shows that Eurocode design is not consistently conservative, whereas a comparison to the Critical Shear Crack Theory is. The Critical Shear Crack Theory, however, capacity comparison shows large variances. The support condition is not explicitly considered in the current flat slab design for punching shear at elevated temperature, therefore an improved design approach ought to be considered.

NOMENCLATURE

For Eurocode:
$A_{c,y}, A_{c,z}$ = area of the concrete according to the definition of N_{Ed} (mm^2)
$C_{Rd,c}$ = Country National Annex specific factor
$N_{Ed,y}, N_{Ed,z}$ = longitudinal forces across the full bay for internal columns and the longitudinal force across the control section for edge columns. The force may be from a load or pre-stressing action. (N)
$v_{Rd,c}$ = design punching shear resistance of a slab without shear reinforcement along the control section (MPa)
d = effective slab depth (mm)
f_{ck} = characteristic compressive cylinder strength of concrete at 28 days (MPa)
k_1 = punching shear factor
γ_c = partial factor for concrete
ρ_l = average reinforcement ratio for longitudinal reinforcement
ρ_{ly}, ρ_{lz} = relate to the bonded tension steel in the y- and z-directions, respectively. The values should be calculated as mean values taking into account a slab width equal to the column width plus 3d each side.
σ_{cp} = average compressive stress in the concrete from axial load (MPa, compressive positive)
$\sigma_{c,y}, \sigma_{c,z}$ = normal concrete stresses in the critical section in y- and z-directions (MPa, compression positive)

For CSCT failure criterion:
V_R = shear strength (N)
b_0 = control perimeter set at $\frac{d}{2}$ of the border of the support region and circular at the corners (mm)
d_v = shear-resisting effective depth (mm)
d_{g0} = reference aggregate size (16 mm)
d_g = maximum aggregate size (mm)
w = critical shear crack width (mm)
ψ = slab rotation
d = effective depth of the member (mm)

For CSCT load-rotation curve:
V = shear failure load (N)
V_{flex} = shear force associated with flexural capacity of slab specimen (N)
m_R = nominal moment capacity per unit width (N)
ρ = flexural reinforcement ratio
f_y = flexural reinforcement yield strength (MPa)
d = distance from extreme compression fibre to the centroid of the longitudinal tensile reinforcement (mm)

f_c = average compressive cylinder strength of concrete (MPa)
r_s = radius of circular isolated slab element (mm)
r_q = radius of the load introduced at the perimeter (mm)
r_c = radius of circular column (mm)
ψ = slab rotation
E_s = flexural reinforcement Young's modulus (MPa)

1. INTRODUCTION

The collapse of the Gretzenbach (Switzerland) underground car park following fire [1] triggered concerns over the punching shear capacity of flat slabs at elevated temperatures. Shear behaviour in concrete at ambient temperature is complex, despite being a well-researched area. There is even less knowledge about shear in concrete subjected to thermal gradients, with only a few experimental studies having been conducted [2-5]. There is growing recognition that the shear behaviour of concrete in fire is dependent on the effects of in-plane actions that result from restrained thermal expansion, large deflection load-carrying mechanisms, and degradation of material properties.

The current Eurocode [6] design of flat reinforced concrete floor slabs for fire conditions uses the ambient design approach, with different prescriptive methods (500°C Isotherm and Zone method) to decrease the cross-sectional geometry according to the temperature penetration of the fire. Additionally, each material strength is degraded to account for elevated temperature. Alternatively, performance based design can be used.

Eurocode clause 2.4.2 Member analysis, states that "(*4) Only the effects of thermal deformations resulting from thermal gradients across the cross-section need be considered. The effects of axial or in-plane thermal expansions may be neglected. (5) The boundary conditions at supports and ends of member, applicable at time t=0, are assumed to remain unchanged throughout the fire exposure*" [6]. This approach has the potential danger that boundary conditions or large displacement mechanisms are not considered. Each reinforced-concrete element is designed for fire in isolation, rather than considering the whole structural interaction of a building.

The drawbacks of the current Eurocode punching shear design for elevated temperature is criticised in [7], which states that "*the aforementioned [ambient design] code equations were obtained on a semi-empirical basis, by operating a regression of the available experimental data: an immediate extension of these expressions to the case of fire is, therefore, highly questionable, to say the least.*"

In 2009, [8] outlined their concerns regarding "*indirect effects ensuing from the redistribution of the internal forces*" on punching shear in fire. The indirect actions are assessed by modelling a fire scenario of an underground car park and [9] found that "*the fire scenario has an important impact on the increase of the axial load*".

This paper presents the experimental findings from fifteen different slab-column specimens in punching shear subjected to fire. These tests are the first to have compared the effects of different support conditions, aiming to replicate whole structural behaviour. A purpose-built reaction frame allowed the support conditions of the specimens to be either simply-supported or restrained against axial expansion and rotation. Slab thickness and reinforcement ratio were also investigated. Load was applied to a column stub and the slabs were heated using an array of propane gas radiant panels.

2. EXPERIMENTAL PROGRAMME

Fifteen flat slab specimens, 1400 by 1400 mm with central column stubs were tested in punching shear at both ambient and elevated temperatures. The slab support type, thickness, and reinforcement ratio were altered as detailed in Table 1. No shear reinforcement was provided and the orthogonal flexural reinforcement was based on the ambient design methods of [10]. The test configuration, instrumentation, specimens and sequence are detailed in [11].

A purpose-built reaction frame allowed the boundary support conditions to be altered. As shown in Figure 1, the support conditions were either restrained (fixed against in-plane expansion

and edge moment), or unrestrained (allowed to expand, and free to rotate). The test arrangement is shown in Figure 2.

Table 1.
Test programme and geometric characteristics of the slab-column specimens.

Specimen ID	Fire scenario	Support type	Slab thickness (mm)	Flexural reinforcement ratio (%)	Reinforcement diameter ⌀ and spacing (mm)
AU50-0.8	Ambient	Unrestrained	50	0.8	6⌀ at 114
AU75-0.8	Ambient	Unrestrained	75	0.8	6⌀ at 65
AU100-0	Ambient	Unrestrained	100	0	-
AU100-0.8	Ambient	Unrestrained	100	0.8	6⌀ at 42
AU100-1.5	Ambient	Unrestrained	100	1.5	8⌀ at 42
HU50-0.8	Heated	Unrestrained	50	0.8	6⌀ at 114
HU75-0.8	Heated	Unrestrained	75	0.8	6⌀ at 65
HU100-0	Heated	Unrestrained	100	0	-
HU100-0.8	Heated	Unrestrained	100	0.8	6⌀ at 42
HU100-1.5	Heated	Unrestrained	100	1.5	8⌀ at 42
HR50-0.8	Heated	Restrained	50	0.8	6⌀ at 114
HR75-0.8	Heated	Restrained	75	0.8	6⌀ at 65
HR100-0	Heated	Restrained	100	0	-
HR100-0.8	Heated	Restrained	100	0.8	6⌀ at 42
HR100-1.5	Heated	Restrained	100	1.5	8⌀ at 42

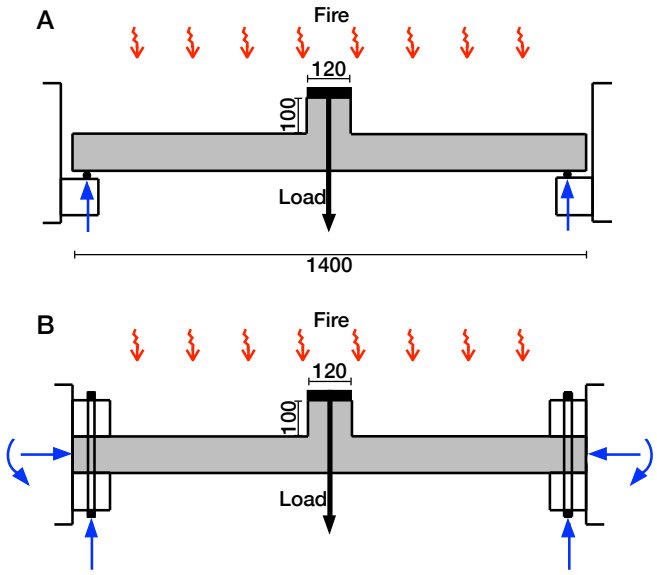

Figure 1
Schematic of the test support conditions (showing A. unrestrained and B. fully restrained).

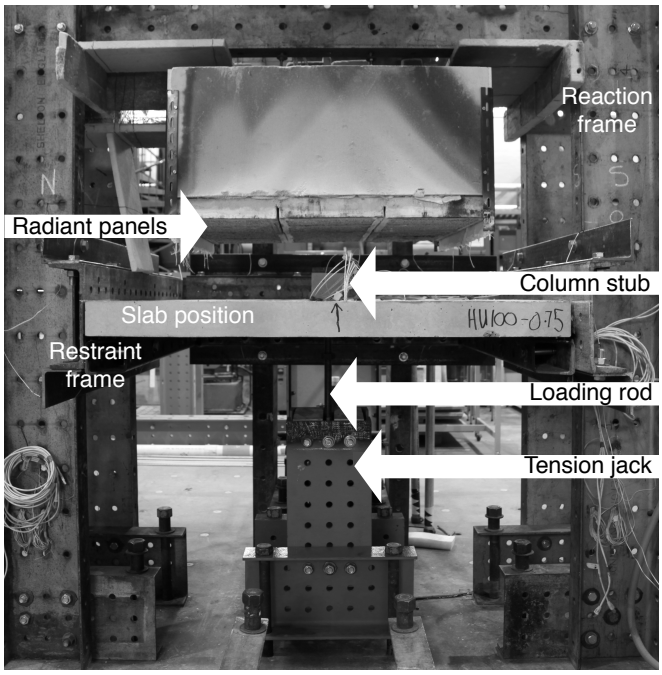

Figure 2
Heated test setup with the insulation removed.

3. EXPERIMENTAL RESULTS

The test series results are presented in detail in [11], with key results shown in Table 2. The

ambient slabs were continuously loaded to failure. The heated specimens were loaded to 70% of their respective ambient capacity (in accordance with Eurocode 1-2 [6]). This load was held constant, whilst the slabs were heated for two hours. The slabs that failed during the two hours heating were immediately unloaded. The applied load was maintained on the specimens that did not fail, whilst they were allowed to cool until temperatures throughout the depth dropped below 150°C. Residual strength tests were conducted the following day on these specimens.

Table 2.
Ambient and residual test results.

Specimen ID	Failure load (kN)	Residual capacity (kN)	Burn time (min)
AU50-0.8	54.2	-	-
AU75-0.8	101.4	-	-
AU100-0	43.8	-	-
AU100-0.8	226.3	-	-
AU100-1.5	279.7	-	-
HU50-0.8	-	55.7	120
HU75-0.8	-	90.7	121
HU100-0	38.9	-	6
HU100-0.8	174.8	-	4
HU100-1.5	237.0	-	14
HR50-0.8	-	64.4	121
HR75-0.8	-	115.5	120
HR100-0	-	82.2	99
HR100-0.8	-	245.1	120
HR100-1.5	233.2	-	105

4. ANALYSIS AND DISCUSSION

This section compares the Eurocode 2 design punching shear capacity for both ambient and elevated temperature to the experimental results. The critical shear crack theory (CSCT) is also compared to the experimental results. This is an ambient model, but its predictions have been modified by reducing the concrete and steel properties according to Eurocode 2, Part 1-2 material properties at elevated temperature.

4.1 EUROCODE 2 DESIGN PUNCHING SHEAR CAPACITY

The ambient temperature punching shear stress design resistance of slabs without shear reinforcement is given by Equation 1 [12].

$$v_{Rd,c} = C_{Rd,c}k(100\rho_l f_{ck})^{1/3} + k_1\sigma_{cp} \geq (v_{min} + k_1\sigma_{cp}) \quad \text{(Equation 1)}$$

The only temperature-dependent variable in Equation 1 is the characteristic compressive cylinder concrete strength at 28 days (f_{ck}). The ambient temperature strength was measured to be 51 MPa. Table 3 gives the maximum temperature recorded in each test (at surface level), and the corresponding reduced concrete strength at these temperatures according to [6].

Table 3.
Concrete material properties at elevated temperature (for siliceous concrete)

Specimen ID	Max. temp. (°C)	Characteristic compressive strength	
		Reduction factor	$f_{c,\theta}$, (MPa)
HU50-0.8	500	0.600	30.6
HR50-0.8	630	0.405	20.7
HU75-0.8	480	0.630	32.1
HR75-0.8	560	0.510	26.0
HU100-0.8	130	0.985	50.2
HR100-0.8	435	0.698	35.5
HU100-1.5	208	0.942	48.0
HR100-1.5	510	0.585	29.8

The partial concrete factor is taken as 1 to allow for comparison to the experimental values. Other parameters used in Equation 1 were:
$C_{Rd,c} = 0.18$
$k = 2$
$k_1 = 0.1$
$\sigma_{cp} = N_{Ed}/A_c$ (where N_{Ed} is the in-plane force, equal in both the y and z directions of the slab for this case, and A_c is the slab cross-sectional area)

Table 4 gives further parameters used to calculate the punching shear capacity.

For the unrestrained slab tests, the in-plane force was approximately zero. For the restrained slabs, however, compressive in-plane force developed during heating. The reaction frame was instrumented to measure the boundary reaction in-plane forces and moments during the tests; however, reliable measurements were not obtained. This data however, was used here to make a support type comparison.

Though Eurocode 2 design does not explicitly assess for varying support conditions, it is assumed the second term in Equation 1 is sufficient to make a comparison for both support conditions as the boundary reaction forces are considered by using the unrestrained and restrained experimental boundary reaction forces in the calculation.

To obtain the punching shear capacity (V) from the shear stress resistance ($v_{Rd,c}$) calculated in Equation 1, the area defined by the slab thickness and the punching shear perimeter (u). The punching shear perimeter is calculated using Eurocode 2, Part 1-1 [12] basic control section, which has been linearly extrapolated to the unheated surface.

Figure 3 compares the shear capacities obtained during the experiments with the Eurocode 2 predictions. Upon first inspection, it is concerning that the design code is not consistently conservative. However on closer inspection, Eurocode is not conservative for many of the small, thinner specimens. The 50 and 75 mm thick specimens failed in flexure-shear mechanisms [11], whereas the thicker 100 mm slabs failed in pure shear. Additionally, the thinner specimens are likely to be smaller than those used in formulating the empirical Equation 1, and are potentially affected by size effects [13]. Eurocode shear design predicts shear capacities similar to the measured failure loads for the 100 mm thick slabs, which failed in pure punching shear mechanisms.

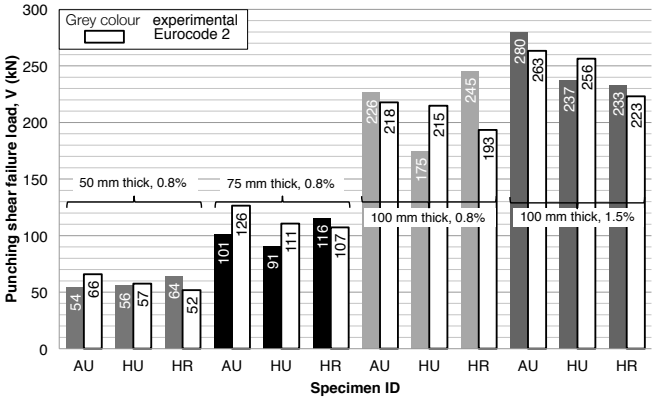

Figure 3
Experimental punching shear capacity compared to the Eurocode 2 design calculation.

Figure 4 gives the ratio of the Eurocode design calculation to the experimentally measured shear capacity (with conservative results < 1.0). The Eurocode calculated capacities for the ambient and elevated temperature tested, 100 mm unrestrained slabs do not vary greatly in Figure 3. This is caused by the heated unrestrained slab-column specimens having failed soon after ignition, therefore the concrete strength is not significantly degraded prior to failure. Figure 4 shows the respective difference between the two support cases when at elevated temperature. The unrestrained are consistently not conservative, whereas the restrained are conservatively predicted by Eurocode. It is comforting that the restrained supported slabs are consistently conservatively predicted by Eurocode, as real building supports are probably closer to the restrained than unrestrained support case.

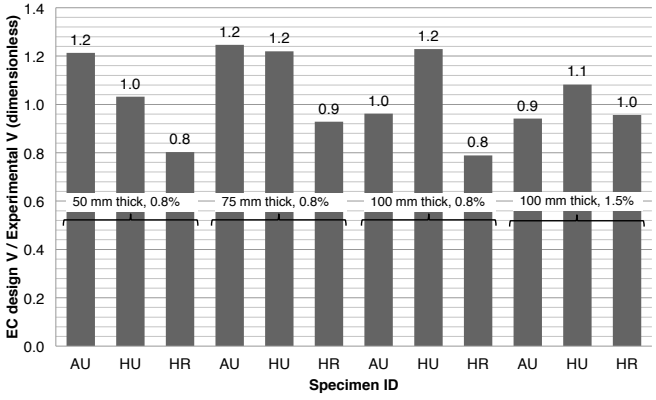

Figure 4
Ratio of Eurocode 2 design shear capacity to experimental punching shear capacity.

Table 4
Eurocode 2 punching shear capacity parameters.

Specimen ID	Average effective depth, d (mm)	ρ_l	N_{Ed} (N)	A_C (mm^2)	σ_{cp} (MPa)	$v_{Rd,c}$ (MPa)	V (kN)
AU50-0.8	35	0.007	2960	70000	0.04	1.19	66
AU75-0.8	62	0.007	6250	105000	0.06	1.19	126
AU100-0.8	83	0.008	27300	140000	0.20	1.25	218
AU100-1.5	81	0.014	12600	140000	0.09	1.52	263
HU50-0.8	31	0.008	-2680	70000	-0.04	1.04	57
HU75-0.8	58	0.007	3670	105000	0.03	1.04	111
HU100-0.8	81	0.008	-1270	140000	-0.01	1.24	215
HU100-1.5	86	0.014	24200	140000	0.17	1.48	256
HR50-0.8	31	0.008	24200	70000	0.35	0.93	52
HR75-0.8	55	0.008	31400	105000	0.30	1.01	107
HR100-0.8	82	0.008	20200	140000	0.14	1.11	193
HR100-1.5	82	0.014	41100	140000	0.29	1.29	223

4.2 CRITICAL SHEAR CRACK THEORY CAPACITY

In [14], Muttoni and Fernàndez Ruiz describe the CSCT proposed for draft 2010 fib Model Code. The authors present an ambient mechanical model that gives consistent and compact design formulations for shear and punching shear in members with and without shear reinforcement, as well as non-symmetrical loading conditions.

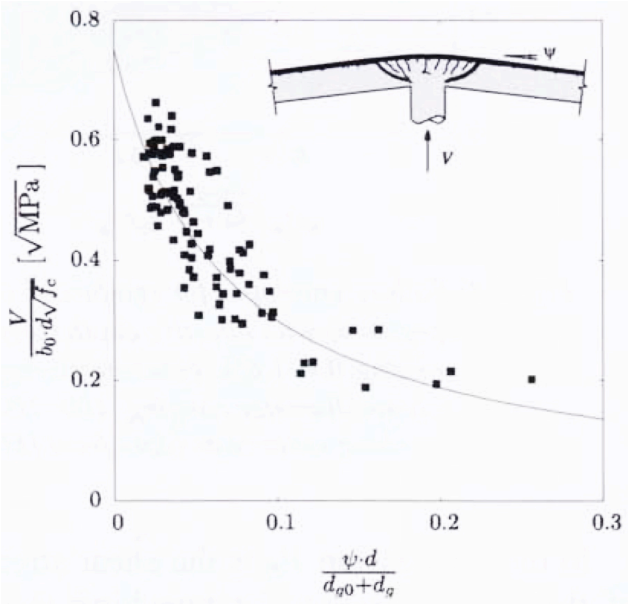

Figure 5
Comparison of 99 experimental test results to Muttoni's CSCT [14].

The CSCT is supported by 146 actual size punching shear tests. Figure 5 shows that there is good agreement between the model and 99 experimental test results, at ambient temperature.

The CSCT is based on a critical crack that penetrates through an inclined concrete compressive strut, which transfers the load on the slab to the column (Figure 6). For members without shear reinforcement, the shear strength is governed by the crack width and roughness of the shear crack. The model is based on kinematic equilibrium equations at failure of the free-body rotation of the slab relative to the column.

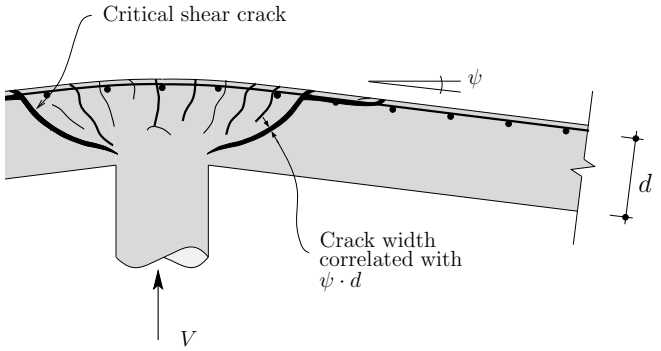

Figure 6
Muttoni's critical shear crack position [15].

Figure 7 shows that the punching shear strength is found at the intersection between the CSCT failure criterion and the load-rotation response of the slab. Muttoni and Fernàndez Ruiz comment that

"*developing suitable moment-curvature and axial force in-plane strains provides a general frame to investigate some phenomena like the increase of the punching shear strength in slabs with restricted horizontal expansion..., the behaviour and strength of flat slabs under fire conditions..., or the increase of the punching shear strength for slabs transferring large column loads*"[14].

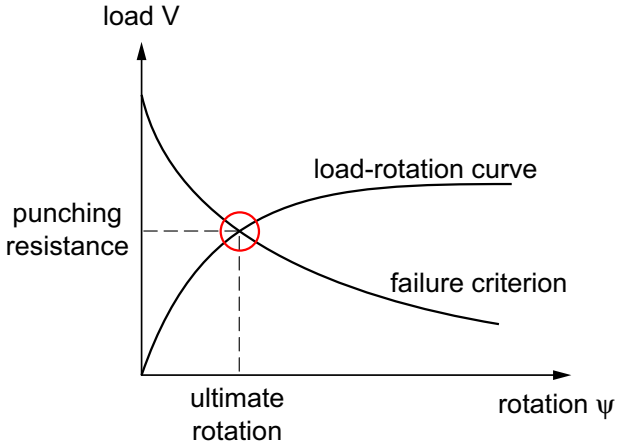

Figure 7
Calculation of the punching shear capacity by Muttoni's CSCT [7].

The CSCT model will here be compared to the unrestrained ambient and elevated temperature test results. The CSCT failure criterion and load-rotation curve for an ambient, unrestrained member without shear stirrups is given by Equations 2 and 3, respectively [16].

Failure criterion:

$$\frac{V_R}{b_0 \cdot d_v \cdot \sqrt{f_c}} = \frac{3/4}{1 + 15\frac{w}{d_{g0} + d_g}}$$

where:

$$w = \psi \cdot d$$

(Equation 2)

Load-rotation curve:

$$V = V_{flex}\left(\frac{\psi}{1.5}\frac{d}{r_s}\frac{E_s}{f_y}\right)^{\frac{2}{3}}$$

where:

$$V_{flex} = 2\pi m_R \frac{r_s}{r_q - r_c}$$

$$m_R = \rho f_y d^2\left(1 - \frac{\rho f_y}{2f_c}\right)$$

(Equation 3)

The load-rotation curve assumes the slab specimens are circular; however, it can be modified with Equation 4, as outlined by [17], to consider rectangular slab sections.

$$r_{a,eq} = \frac{2b}{\pi} \quad , \quad r_{Q,eq} = b_Q$$

where for this analysis:
$r_{a,eq} = r_c$ = radius of circular column (mm)
$r_{Q,eq} = r_q$ = radius of the load introduced at the perimeter (mm)
b = column width (mm)

(Equation 4)

The variables in the CSCT that would vary with temperature are the concrete characteristic compressive cylinder strength (f_c), the flexural reinforcement yield strength (f_y) and Young's modulus (E_s). Table 5 gives the ambient steel properties measured.

Table 5
Ambient flexural reinforcement properties.

Ribbed reinforcement diameter (mm)	Type of steel	f_y (MPa)	E_s (GPa)
6	cold worked	549.6	200
8	hot rolled	571.1	222

The ambient steel yield strength and Young's modulus were reduced according to the maximum test temperature, to give elevated temperature properties that were used in the CSCT calculations. The Eurocode 2 class X reduction factors were used.

Other variables used in the calculations that were common to all the tests were:
b = 120 mm
r_q = 655 mm
r_s = 700 mm
r_c = 76 mm
d_g = 10 mm
width of the slab = 1400 mm

Table 6
Elevated temperature steel properties, calculated using the Eurocode 2 class X reduction factors.

Specimen ID	Max. temp (°C)	Reduction factors		Reduced values	
		$f_{sy,\theta}$ (MPa)	$E_{s,\theta}$ (MPa)	$f_{sy,\theta}$ (MPa)	$E_{s,\theta}$ (GPa)
HU50-0.8	350	0.95	0.825	522	165
HR50-0.8	445	0.81	0.683	445	136
HU75-0.8	245	1.00	0.928	549	185
HR75-0.8	290	1.00	0.905	549	181
HU100-0.8	18	1.00	1.000	549	200
HR100-0.8	170	1.00	0.965	549	193
HU100-1.5	22	1.00	1.000	571	222
HR100-1.5	148	1.00	0.976	571	216

Table 7
Critical shear crack theory failure criterion parameters.

Specimen ID	Slab thickness (mm)	Average concrete cover (mm)	Reinforcement diameter (mm)	d (mm)	b_0 (mm)	f_c (MPa)
AU50-0.8	50	9	6	35	590	51.0
AU75-0.8	75	7	6	62	675	51.0
AU100-0.8	100	11	6	83	741	51.0
AU100-1.5	100	11	8	81	734	51.0
HU50-0.8	50	13	6	31	577	30.6
HU75-0.8	75	11	6	58	662	32.1
HU100-0.8	100	13	6	81	734	50.2
HU100-1.5	100	6	8	86	750	48.0

Table 8
Critical shear crack theory load-rotation parameters.

Specimen ID	No. rebars in each orientation	ρ	f_y (MPa)	m_R (N)	V_{flex} (kN)	E_s (GPa)
AU50-0.8	12	0.007	550	4,540	34.5	200
AU75-0.8	21	0.007	550	14,100	107.0	200
AU100-0.8	33	0.008	550	29,500	224.0	200
AU100-1.5	33	0.015	571	51,100	388.0	222
HU50-0.8	12	0.008	522	3,730	28.3	165
HU75-0.8	21	0.007	549	12,900	97.8	185
HU100-0.8	33	0.008	549	28,800	219.0	200
HU100-1.5	33	0.014	571	53,800	409.0	222

Tables 7 and 8 give the parameters involved in calculating the punching shear capacity (see Equations 2, 3 and 4). Figures 8 show the intersecting capacity and load-rotation curves that define the ambient temperature punching shear capacities; whilst Figure 9 shows those for the elevated temperature capacities. The elevated temperature decreases the steel stiffness, thereby decreasing the shear capacity for equivalent slab rotation angles.

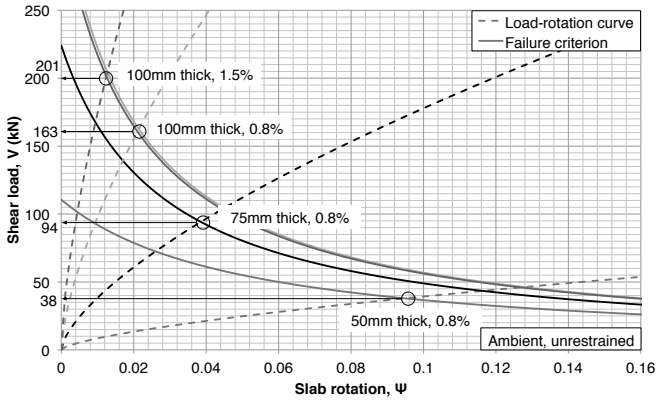

Figure 8
Ambient CSCT punching shear capacity curves.

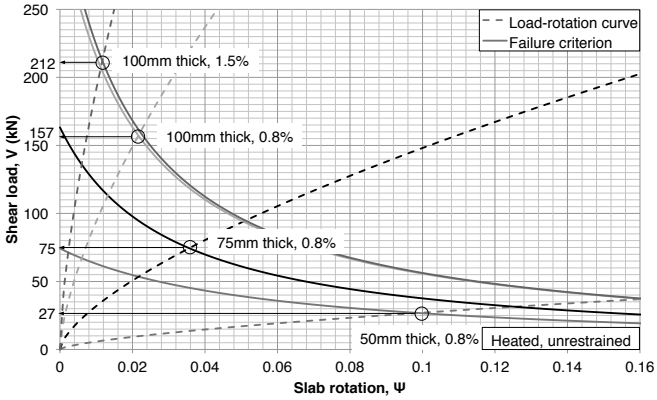

Figure 9
Elevated temperature CSCT punching shear capacity curves.

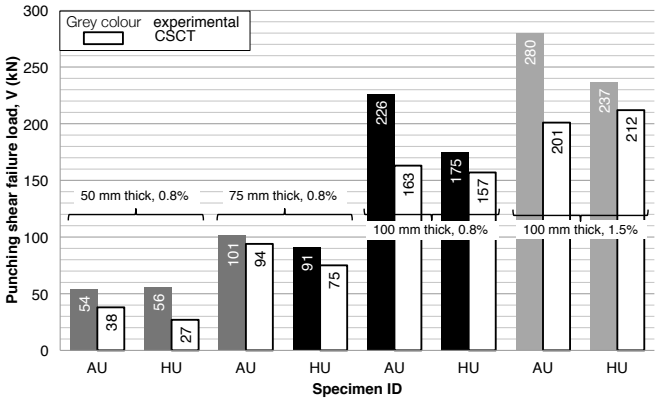

Figure 10
Experimental punching shear capacity compared to CSCT.

Figure 10 compares the CSCT capacities calculated compared to the unrestrained slab-column experimental values. The 100 mm specimen comparison shows that the model has large differences when compared to the experimental values. However, these variations are within the scatter shown in Figure 5.

The CSCT has been applied to the heated tests by simply degrading the steel and concrete material properties using the Eurocode reduction factors and recorded temperatures. However, this does not consider the restrained thermal stresses and in-plane axial forces, which require a more detailed re-evaluation of the mechanics in the CSCT at higher temperatures.

5. CONCLUSIONS

Fifteen model slab-column punching shear specimens were tested at either ambient or elevated temperature. The boundary support conditions of the specimens were altered to be either fully restrained or unrestrained.

This paper presents a comparison of the experimental capacities from the punching shear test series to the Eurocode design method, following the method for elevated temperature design. The paper also compares the results to Muttoni's critical shear crack theory, which is modified for elevated temperatures by degrading the material properties.

The smaller (50 and 75 mm thick) specimens failed in flexure-shear mechanisms rather than pure punching shear, unlike the 100 mm thick slab-columns. Eurocode design was not conservative for the thinner specimens. The results demonstrated that with regard to the 100 mm thick specimens, Eurocode design was only conservative for the restrained condition and not the unrestrained.

A comparison to the critical shear crack theory shows that it is consistently conservative in comparison to the experimental results. The model has large capacity variances for the 100 mm thick specimens, although these are consistent with the original comparison with test data. More detailed consideration is required of the effects of restrained thermal expansion in the model.

ACKNOWLEDGEMENTS

This PhD project was supported by funding from the EPSRC, together with additional follow-up funding provided by EPSRC and AECOM.

REFERENCES

1. [Muttoni, A., Fürst, A., and Hunkeler, F.],[2005] '[Deckeneinsturz der tiefgarage am Staldenacker in Gretzenbach]', [*Medieninformation vom 15.11.2005.*]
2. [Kordina, K.],[1997] '[Über das Brandverhalten punktgestützter Stahlbetonplatten (On the Fire Behaviour of Reinforced Concrete Flat Slabs)]', [*Deutscher Ausschuss für Stahlbeton (DAfStb), Berlin (Germany), Heft 479, p.106*]
3. [Annerel, E., Lu, L., Taerwe, L.],[2013] '[Punching shear tests on flat concrete slabs exposed to fire]', [*Fire Safety Journal, Vol.57, pp.83-95*]
4. [Salem, H., Issa, H., Gheith, H., and Farahet, A.],[2012] '[Punching shear strength of reinforced concrete flat slabs subjected to fire on their tension sides]', [*HBRC Journal, Vol.8 Issue. 1, pp.36-46*]
5. [Ghoreishi, M., Bagchi, A., and Sultan, M.A.],[2013] '[Review of the punching shear behaviour of concrete flat slabs in ambient and elevated temperature]', [*Journal of Structural Fire Engineering, Vol.4 Issue.4, pp.259-279*]
6. [BSI],[2004] '[BS EN 1992-1-2:2004: Eurocode 2: Design of concrete structures, Part 1-2: General rules-Structural fire design]', [*European Committee for Standardisation*]
7. [Bamonte, P., Fernàndez Ruiz, M., and Muttoni, A.],[2012] '[Punching shear strength of R/C slabs subjected to fire]', [*In 7th International Conference on Structures in Fire, Zurich, Switzerland, June 6-8, 2012, pp.689-698*]
8. [Bamonte, P., Felicetti, R., and Gambarova, P.],[2009] '[Punching shear in fire-damaged reinforced concrete slabs]', [*American Concrete Institute, Vol.265, pp.345-366*]
9. [Annerel, E., Taerwe, L., Merci, B., Jansen, D., Bamonte, P., and Felicetti, R.],[2013] '[Thermo-mechanical analysis of an underground car park structure exposed to fire]', [*Fire Safety Journal, Vol.57, pp.96-106*]
10. [Guandalini, S., Burdet, O., and Muttoni, A.],[2009] '[Punching tests of slabs with low reinforcement ratios]', [*ACI Structural Journal, Vol.106 Issue.10, pp.87-95*]
11. [Smith, H.K.M., Stratford, T.J., and Bisby, L.A.],[2014] '[Punching shear of restrained reinforced concrete slabs under fire conditions]', [*In 8th International Conference on Structures in Fire, Shanghai, China, June 11-13, 2014, pp.443-450*]
12. [BSI],[2004] '[BS EN 1992-1-1:2004: Eurocode 2: Design of concrete structures, Part 1-1: General rules and rules for buildings]', [*European Committee for Standardisation*]
13. [Bažant, Z., and Cao, Z.],[1987] '[Size effect in punching shear failure of slabs]', [*ACI Structural Journal, Vol.87 Issue.1, pp.44-53*]
14. [Fédération international du béton (*fib*)],[2010] '[Shear and punching shear in RC and FRC elements]', [*fib Bulletin 57, Salò, Italy, p.268*]
15. [Fernàndez Ruiz, M., and Muttoni, A.],[2010] '[Performance and design of punching shear reinforcing systems]', [*In 3rd fib International Congress, Washington DC, USA, 2010*]
16. [Muttoni, A.],[2008] '[Punching shear strength of reinforced concrete slabs without transverse reinforcement]', [*ACI Structural Journal, Vol.105 Issue. 4, pp.440-450*]
17. [Guandalini, S.],[2005] '[Poinçonnement symétrique des dalles en béton armé]', [*PhD thesis, École Polytechnique Fédérale de Lausanne*]